J Fail. Anal. and Preven.
https://doi.org/10.1007/s11668-022-01417-6

TECHNICAL ARTICLE—PEER-REVIEWED

Investigating the Effects of H_2O Interaction with Rainscreen Façade ACMs During Fire Exposure

L. Casey · S. Simandjuntak · J. Zekonyte · J. M. Buick · A. Saifullah

Submitted: 8 March 2022 / Accepted: 10 May 2022

Abstract Preliminary investigations into adverse reactions between aluminum alloy sheets, used as facings for aluminum composite material rainscreen panels, and water vapor ($2Al + 3H_2O -> Al_2O_3 + 3H_2$) contributing to high-rise façade fire events are reported. Panels containing a PE blend (70% polyethylene 30% calcium carbonate) core were characterised and subsequently exposed to a surface irradiance of 50 kW/m^2 using a cone calorimeter, in modified ISO 5660:1/ASTM 1354 procedures, involving water spray. Inverse modeling techniques were applied to determine the effects of water spray on the samples' combustion parameters. From the current study, evidence for the liberation of diatomic hydrogen (H_2) contributing to peak heat release rate during combustion was not found. Observed thermal shock and subsequent degradation led to a greater surface area exposure of combustible inner core material, contributing to an increase for both peak heat release rate (from 393 kW/m^2 to 1040 kW/m^2) and total energy release (97 MJ/m^2 to 117 MJ/m^2). Findings suggest no significant increase in the combustibility of aluminum composite panels arises through reduction–oxidation reactions between aluminum-water at 50 kW/m^2 irradiance. However, thermomechanical processes, brought upon by environmental conditions and external intervention, may affect the dynamic combustion behavior of aluminum composite panels.

L. Casey (✉) · S. Simandjuntak · J. Zekonyte · J. M. Buick · A. Saifullah
School of Mechanical and Design Engineering, University of Portsmouth, Anglesea Building, Portsmouth PO1 3DJ, UK
e-mail: Laurence.casey@portsmouth.ac.uk

Keywords Rainscreen façade · Combustion · Aluminum composite material · Fire dynamics simulator · Reduction–oxidation reactions

Introduction

Cumulative reports of extreme high-rise façade fire events in the last two decades [1] have resulted in continuing developments in fire safety engineering research, with prominent focus on the reaction-to-fire nature of commonly used façade materials during flame exposure [2–11], due to the identified potential for fire spread along the exterior of a building, with subsequent interior re-entry at fenestration component locations, overcoming the desired compartmentation effect. Aluminum composite material (ACM) panels with a high polymer, such as polyethylene (PE), content, used for rain screen cladding applications, have been a common factor among many examples. Nevertheless, limited research has been conducted on the risks associated with discrete chemical interactions that may lead to thermal runaway, such as metal-water reactions, and thermomechanical failure of individual composite elements, affecting the overall combustion behavior.

McKenna et al. [9] used a combination of micro- and bench-scale fire tests to investigate the reaction-to-fire behavior of different types of façade products, including various ACM variants. Panels with a 100% weight Low-Density PE (LDPE) core showed 55× greater peak heat release rates (pHRR) at 1364 kW/m^2 and 70× greater total heat release (THR) at 107 MJ/m^2, compared to the highest performing ACM under review. The novel methods described in the study allowed the ACM core material to ignite, without prior failure of the aluminum facing,

Published online: 20 May 2022

ensuring the cores true combustion potential could be observed and recorded. Guillame et al. [4] used intermediate scale tests to review the performance of assembled façade systems adopting rainscreen cladding panels. ACM PE samples gave exceptionally dissimilar results from the other solutions tested, especially in terms of heat release rate, supporting the assumption that higher polymer content will lead to increased fire hazard. Srivastava, Nakrani & Ghoroi [12] presented data collected from the same bench-scale tests used by McKenna et al. [8] on ACM PE samples, with the aluminum facing fully intact without initially exposing the core to the surroundings. A pHRR of 351 kW/m^2 was recorded for samples exposed to 50 kW/m^2 irradiance, which is around 25% of the value found by McKenna et al. [9]. This suggests the failure or disruption of the ACM facing is relevant to the dynamic heat release observed, and that the presence of an alloy sheet facing will reduce pHRR during cone calorimeter experiments.

The aluminum alloy sheets used as facings for ACMs, typically made using AW 5005A (AlMg1) H22/H42, alloys, are assumed to provide no contribution to a fire by combustion [13]. Aluminum is not expected to combust during a typical building fire scenario. Possessing protective oxide layers protects the metal from rapid oxidation (combustion) below the melting point of alumina at approx. 2000 °C. Unsurprisingly, when tested to ISO 1182:2020 [14] or ASTM 136-19a [15] which involves exposing a small sample to a vertical tube furnace held at 750 °C, negligible, and often negative, heat rise is observed [16, 17]. Aluminum melts at this temperature but does not burn. For this reason, aluminum is assumed to have no effect on combustion of façade system, except through shielding the combustible inner core, delaying ignition of rainscreen panels, until it is disrupted, deboned from the core material, or removed from the construction assembly. Khan et al. [1] reviewed the combustion behavior of two other ACM variants (namely FR and A2) exposed to a cone calorimeter of irradiance up to 60 kW/m^2, using vertical sample orientation, with consideration for thermomechanical responses. Results indicate FR and A2 cores can still be ignited above 35 kW/m^2, much lower than the required energy to ignite aluminum and its alloys. Findings highlight the importance of composite panel failure mechanisms, such as layer debonding and bending stresses arising from thermal expansion.

Hypotheses of significant contribution to façade fire behavior, and difficulty in extinguishment, due to exothermic redox processes upon aluminum alloy sheets and H_2O interaction, during high-rise facade fire scenarios, have been suggested in the years since the disaster witnessed at Grenfell Tower in London, 2017 [14, 15, 17, 18]. Harwood [19], for example, proposed that at the Grenfell Tower fire, a breach in aluminum's protective oxide layer, caused by impinging steam, led to the metal reacting with water, liberating hydrogen gas. A similar hypothesis was presented by Maguire and Woodcock [20–22], who extended the reactions to aluminum carbide formation, and subsequent methane gas, upon hydrolysis. A lack of data has precluded reliable evidence to support the suppositions to date.

Reactions between molten aluminum and water have been the focus of a variety of research, based on preventing accidents at aluminum manufacturing/casting plants [23, 24]. Ferocious behavior has been previously reported, in some cases resulting in explosions [25]. In the latest aluminum association's annual summary report on molten metal incidents Aluminum Association [13], 163 explosion incidents were reported for 2019. A total of 170–195 incidents per year were reported in the previous four years. Explosions involving alkali metals and water have been found to occur through different mechanisms, most notably steam-vapor explosions. This is the immediate boiling of water upon contact with hot metallic surfaces, where the rapid phase transformation leads to a shockwave.

Numerical modeling of ACMs exposed to fire can be approached in several ways but is generally considered an area of ongoing research. Work by McKenna et al. [9] and Guillaume et al. [3–5] demonstrate modeling assumptions that include the removal of aluminum at a defined threshold temperature, such as conservatively at 550^{o}C, replicating structural failure or the facing detaching from the inner core. The core material of the ACM is assumed to contain the lone fuel, which therefore simplifies the models. Validation has been presented by Drean et al. [6], which supports this logic being applied. Experimental data can be successfully simulated using numerical models, with close agreement between predicted and measured kinetics, utilising Arrhenius-based reaction rate solvers, and the relevant material properties defined [26, 27]. It is noted that procedures adopted in the state-of-the-art fire modeling do not consider redox reactions between metallic components and moisture by default and are not found to be incorporated in any relevant façade fire modeling, or appropriate experimental methods, in published literature to date.

Despite this work, gaps in literature for appropriate modeling of the time-dependent dynamic thermomechanical behavior of composite sandwich panels, subjected to elevated temperatures and environmental conditions, experienced throughout building fire scenarios, still exist. This study focuses on preliminary investigations into hypothesised adverse reactions on aluminum composite sandwich panel samples, intended for rainscreen cladding assemblies, via reduction–oxidation reaction with H_2O species, in terms of exothermic response and material integrity degradation. Indicative cone calorimeter experiments using aluminum composite sandwich panel samples,

containing a > 99% low-density polyethylene core (ACM PE), are reported. Data are presented in terms of peak heat release rate (pHRR), effective heat of combustion, total energy release and mass loss per sample. Modifications to ISO 5660:1/ASTM 1354 [28, 29] test standards, by introducing simulated environmental conditions, are reported. Inverse numerical modeling techniques were then developed using Fire Dynamics Simulator (FDS) [30], accompanied by PyroSim GUI [31], to analyze the collected experimental data and develop predictions for the change in combustion behavior of the ACM samples exposed to water spray.

Methods

Materials

An aluminum alloy composite rainscreen panel variant, with a 99%+ weight polyethylene core (ACM PE), is reviewed in this study. The relevant material properties are described in Table 1.

Thermogravimetric Analysis (TGA)

TGA experiments were performed in accordance with ISO 11358:1 [32] using TA Instruments Q50 apparatus, on samples taken from the core of ACM PE panels.

A nitrogen atmosphere was selected to derive the decomposition kinetics using the procedures set out in ISO 11358:2 [33] 11358:3 [34] without combustion at heating rates of 10, 15, 20, 25 and 30 °C/min. The resulting kinetic triplets (activation energy, pre-exponential factor and reaction order) are used in combination with the properties listed in Table 1, as input parameters for numerical modeling.

Cone Calorimeter

Experimental procedures in accordance with ISO 5660:1 and ASTM 1354 [28, 29] were performed on ACM PE panel samples measuring 100 × 100 × 4 mm to establish pyrolysis and combustion behavior. A constant irradiance level of 50 kW/m^2 was selected for all the samples' surface exposure. This is a typical value used when assessing building materials' reaction-to-fire performance [35]. A steel retainer frame was used to hold the sample as the material is not likely to maintain integrity, due to the low melting point of the core material (110 °C), as shown in Table 1. Samples were first wrapped in aluminum foil (excluding the outer facing), with insulated backing using silica wool, as per ISO 5660/ASTM 1354 recommendations. Results for heat release rate, heat of combustion, total energy release and mass loss values are recorded.

ISO 5660:1 Test Variation

The intention of this experiment is to identify any negative change to material performance post water injection. In terms of combustion, hypothetically, if there is no adverse reaction, water should only act to cool the sample's surface, before evaporating away, displacing oxygen. Heat release rate and total energy release decrease as a result of both lower oxygen concentration and lower surface temperatures. To simulate interaction between H_2O species and aluminum components during developed fire exposure, at a flow velocity relative to fire-driven flow through a cavity (around 2 ms-1), an additional variable was introduced to the equivalent conditions used in the standard ISO 5660:1 test procedure, using a dispenser syringe to apply external H_2O onto the sample, at a controlled volume (5 mL per application) and approximate velocity. Using the principles of conservation of mass, the approximate velocity, $v(\mathrm{ms}^{-1})$, of the water exiting the syringe is calculated via Eq 1:

$$v = \frac{V}{At} \quad \text{(Eq 1)}$$

A = Area of opening (2.3 mm^2), V = volume (held constant at 5 mL) and t = application time (s).

An application speed of 2–3 s onto the sample surface for the 5 mL water is optimal to replicate the smoke

Table 1 Properties of materials

Material	Polyethylene (PE)	Polyvinyl difluoride (PVDF)	Aluminum alloy 5005 (Sheet)	Methyl-methacrylate (Assumed)
Type:	Core	Coating	Facing	Adhesive
Thickness	3mm	30 µm	0.5 mm	120 µm
Density	915 kg/m^3	1780 kg/m^3	2700 kg/m^3	940 kg/m^3
Composition	C_2H_4	$(C_2H_2F_2)n$	AW-Al Mn_1, $Mg_{0.5}$	$C_5H_6O_2$
Melting point	110°C	170°C	650°C	− 44°C
Thermal conductivity	0.33 W/K-m	0.18 W/K-m	205 W/K-m	0.13 W/K-m
Specific heat capacity	1.9 kJ/(kg k)	1.4 kJ/(kg/K)	0.9 kJ/(kg-K)	0.19 kJ/(kg-K)

velocity in a façade cavity. 5 mL water is applied in 90 s intervals using a syringe dispenser, at a predicted velocity of 2 ±0.3 ms^{-1}

Pyrolysis and Combustion Modeling

To derive activation energy (*Ea*) and pre-exponential factor (*A*), deconvolution of the experimental derivative thermogravimetric (DTG) curve $\frac{d\alpha}{dT}$ is performed on FDS v6.7.6 [36], using the peak reference temperature, pyrolysis range and heating rate obtained from the experiments as an interface [37], where α = fractional mass loss $(\frac{m_t - m_f}{m_0 - m_f})$, T = temperature (K), m_t = mass at time t (g), m_f = final mass (g)

The relationship between reaction rate and temperature can be expressed as follows:

$$\frac{d\alpha}{dT} = \frac{A}{\beta} e - Ea/RTf(\alpha) = rj(\text{pyrolysis reaction rate}) \quad \text{(Eq 2)}$$

where $f(\alpha) = (1 - \alpha)\ n$ and $\beta = \frac{dT}{dt}$ is the heating rate (K min^{-1}).

To validate the derived kinetic properties, the predicted and experimental TGA curves are compared. Parameterisation techniques are applied to improve accuracy of the data [38].

Inverse Modeling Framework for Modified Cone Experiments using FDS

A coupled experimental modeling data solution was developed and applied, to determine the effects of water spray on the pyrolysis and combustion parameters of ACM samples, during simulated fire exposure, in a controlled environment.

Using experimental cone calorimeter data as input values for FDS, in the form of a HRR vs time ramping function, inverse derivations of predicted pyrolysis and combustion properties can be extracted, using Eq 3:

$$\dot{m}''_f \frac{f(t)\dot{q}''_{user}}{\Delta h_c} \quad \text{(Eq 3)}$$

where $\dot{m}''_f$= rate of fuel mass generation, $f(t)$ = time ramping function (s), $\dot{q}''_{user}$ = experimental HRR (kW/m^2) and Δh_c= average heat of combustion (MJ/kg). A second ramping function, for mass loss rate (MLR), is then used to validate the model, through comparison of the FDS predicted and experimentally recorded heat release rate, considering Eq. 4:

$$HRR = \dot{m}''_f \cdot \Delta h_c \quad \text{(Eq 4)}$$

With the assumption of polyethylene as a lone fuel, thereby excluding aluminum from the simulation, differences in the result between the standard cone calorimeter experiments are compared with the modified cone calorimeter experiment involving water spray.

Results and Discussion

TGA experiments were conducted on ACM PE core samples to characterise the core polymer composition, obtain activation energy, pre-exponential factor and reaction order for pyrolysis modeling on FDS.

In contrast to the material data sheet, a core composition of 70% PE:30% $CaCO_3$ (calcium carbonate) was found. $CaCO_3$ is a common filler material, providing improved mechanical performance to PE blends, while also reducing volatile content, and therefore heat released.

A close agreement between simulated TGA using FDS and experimental values are shown in Fig. 1. This allowed for confidence in the kinetics of the material being represented by FDS and validates the correct volatile release percentage has been identified. Values obtained for polyethylene decomposition via deconvolution are 197 kJ/mol for activation energy and 1.27E12 s^{-1} for the pre-exponential factor, which agrees closely with classical model derivations of 201 kJ/mol using three heating rates, and 193.23 kJ/mol using five heating rates.

For further validation of assumed fuel composition, a mass loss rate ramping function is created using the experimentally recorded sample mass loss values, deriving an FDS predicted heat release rate curve. This curve is then compared with the cone calorimeter's recorded heat release rate, yielding a close relationship, as seen in Fig. 2.

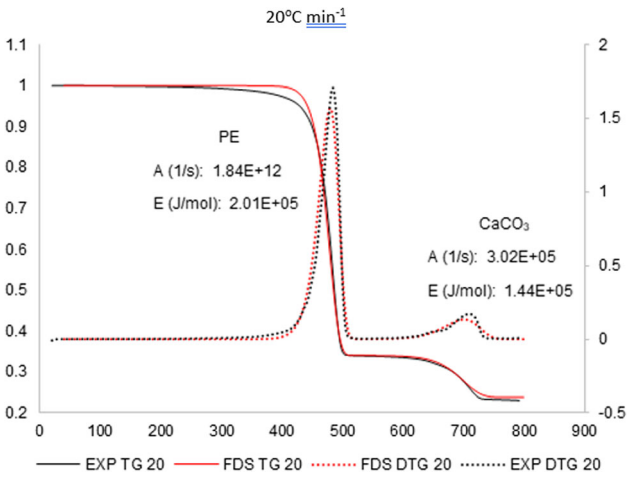

Fig. 1 TGA and DTG curves (FDS) vs experimental (EXP) at 20 °C min^{-1}

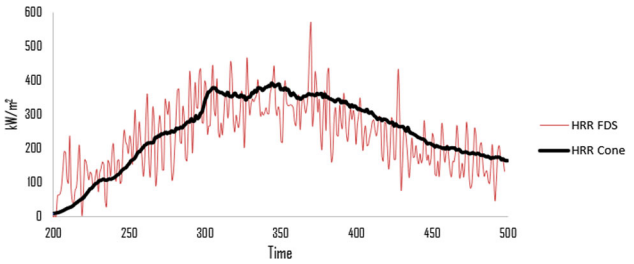

Fig. 2 FDS predicted HRR (red lines) vs cone calorimeter HRR recordings (black line) (Color figure online)

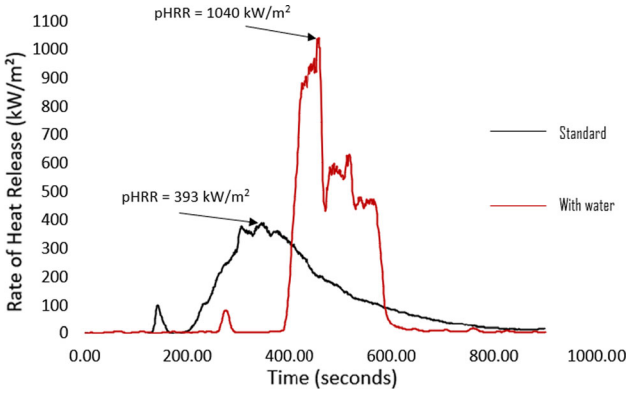

Fig. 3 Cone calorimeter experimental heat release rate vs time, standard (black line) vs with water (red line) (Color figure online)

The recorded heat release rates over time, during the cone calorimeter experiments, are displayed in Fig. 3. There is a clear increase in pHRR (+ 265%) for the sample subjected to water spray. However, delayed ignition was observed for the same sample, lowering the fire growth rate index (FIGRA) value, which is a function of pHRR and time to the pHRR, as shown in Eq 5:

$$\text{FIGRA} = \frac{Q_{pHRR}}{t_{pHRR}} \quad \text{(Eq 5)}$$

where QpHRR = pHRR (kW/m^2) and tpHRR = Time to pHRR (s).

The pHRR falls within the maximum predicted values ($\sim$ 1200 kW/m^2) for neat polyethylene exposed to 50 kW/m^2 irradiance, based on FDS-derived pyrolysis models. Therefore, the results suggest that the differences in heat release may be related to the dynamic thermomechanical behavior of the composite panel, rather than an additional fuel (H_2) being generated. The predicted lone fuel remains as ethylene.

Table 2 summarises the key values derived from the cone calorimeter experiments. A significant increase in peak heat release rate and total energy release is observed for the panel exposed to water spray. It is expected that the sample with higher overall heat release would also achieve higher mass loss, as more fuel is required to supply the additional energy. This was not observed, which initially indicates a new fuel may have been introduced to the system. Additional hydrogen production is expected to increase the average heat of combustion value of the overall material, requiring less sample mass loss to generate the equivalent heat release.

Table 2 Summary of cone calorimeter experimental results

Parameter	Test v1 (standard)	Test v2 (water)
Peak heat release rate	393 kW/m^2	1040 kW/m^2
Average heat of combustion	43.1 MJ/kg	60.3 MJ/kg
Total Energy Release	96.9 MJ/m^2	117 MJ/m^2
Sample Mass loss	2260 g/m^2	1940 g/m^2

This is observed in Table 2, with an average heat of combustion value of 60.3 MJ/kg for the sample exposed to water spray, a 40% increase from the primary sample.

Nonetheless, oxidation of aluminum components leads to a gain in sample mass, as observed in Table 2. This mass increase results in inflation of the derived heat of combustion value, which is calculated by the cone calorimeter software as $\frac{\text{THR}}{\text{TML}}$. The imbalance (from 43.1 to 60.3 MJ/kg) can be justified through aluminum oxidation mass gain, as well as calcium oxide (CaO) hydration, post-$CaCO_3$ decomposition. Water is not absorbed by PE. The mass gain suggests oxidation may have occurred, yet the presence of CaCO, with the ability to gain mass through hydration, reduces the certainty of the source. The molecular weight of alumina is 101.96 g/mol, compared to ($\times$2) 26.98 g/mol for aluminum (53.96 g). Therefore, even small rates of oxidation cause irregularities in the heat of combustion calculation, with negligible contribution to heat release by hydrogen oxidation ($\sim$ 5000 J).

Furthermore, mass gain alone does not verify oxidation occurring because of Al-H_2O interaction; rupture of the oxide layer exposes the substrate to oxidation by air, which may react without producing hydrogen, as seen in reaction 1:

$$4\text{Al}(s) + 3\text{O}_2(g) \rightarrow 2\text{Al}_2\text{O}_3(s). \quad \text{(Eq 6)}$$

With no significant exothermic reaction, water spray delays ignition of samples, as shown by the peak heat release time delay in Fig. 3, and lowers heat release, primarily through the reduction in surface temperature in an endothermic response. However, an increase in combustibility, such as higher values for peak heat release rate, effective heat of combustion and total energy release, signals an adverse reaction to water spray. Considering 0–120s test duration, Fig. 4 shows an initial exothermic response for the sample exposed to water spray, contrasted with a neutral/endothermic response for the standard sample. This heat release rate is insignificantly

relative to the peak heat release rate, and overall energy release, yet suggests evidence of potential metal-water reactivity.

In terms of post-test visual observations, as seen in Fig. 5, in the standard cone calorimeter test, with no water spray, the aluminum facing shows minimal detachment, restricting exposure to the combustible polymer core. The sample exposed to water spray displays signs of enhanced material degradation, exposing a large area of core material, thus producing a higher heat release rate value, through increased rate of pyrolysis. $CaCO_3$/CaCO residue is observed.

To build confidence in the developed inverse modeling analysis, the predicted and experimentally recorded mass loss rates for the primary sample (without water spray) are compared. A close relationship is found between the two, as shown in Fig. 6. The relationship between predicted mass loss rate is derived from a heat release ramp, with the specified fuel C_2H_4, which is released by polyethylene during pyrolysis, leaving no residue (1:1 sample mass to fuel conversion).

The FDS model assumes ethylene fuel is released, with a heat of combustion value of 43.1 MJ/kg. Therefore, at the point of peak heat release, shown in Fig. 3, close agreement between the mass loss rate supports evidence that ethylene is the only fuel present. Following significant hydrogen production, notable discrepancies between the two should appear, with an additional − 285 kJ/mol H_2. Evidence of hydrogen combustion would have been represented by significantly higher FDS predicted mass loss rate compared to the experimentally recorded values during the pHRR, as additional ethylene fuel mass would be required to produce the equivalent heat release.

It was anticipated that the mass loss via water spray evaporation, seen in Fig. 7, would cause irregularities between the two; the FDS model does not account for the water spray. However, the experimentally recorded mass loss is shown in full. These irregular spikes in mass loss can be disregarded from consideration of mass loss rate and heat release since they occurred during water sprays, the average predicted MLR and experimentally recorded MLR are then closely correlated. Following a water spray application at t = 450 s, during the primary combustion phase, a strong endothermic response, resulting in a reduction in heat release rate, is observed.

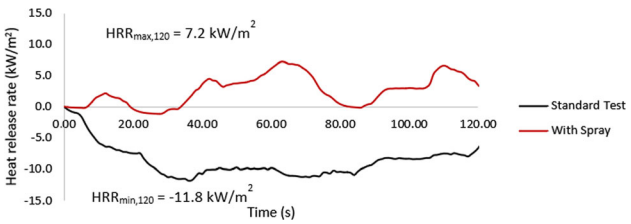

Fig. 4 Cone calorimeter heat release rate recordings for 0-120s, standard test (black line) vs spray (red line) (Color figure online)

Conclusion

Preliminary findings into an investigation of recent hypotheses, related to redox reactions between aluminum alloy facings and water vapor contributing to high-rise building façade fires, are reported. An ad hoc experimental procedure, as well as numerical analysis, was required for the study, as no published methodology, or test standard, could be sourced that directly relates to the scenario in question.

The application of an inverse modeling framework, using FDS, allowed for determination of the effects of water spray on ACM PE samples, during cone calorimeter experiments at 50 kW/m^2 surface irradiance, which appear to be thermomechanical in nature; water spray enhanced degradation of the outer aluminum facing, resulting in exposure of a larger surface area of combustible core material. The dominant failure mechanism assumed is thermal shock.

A close agreement between experimental values and numerical computations was found for fuel generation and heat release rates of ACM PE samples, validating the fuel composition and inverse modeling technique adopted.

For the sample exposed to water spray, an increase of 165% in pHRR and 20% for total energy release was

Fig. 5 Post-test visual observations ACM PE standard test (left) ACM PE modified test (right)

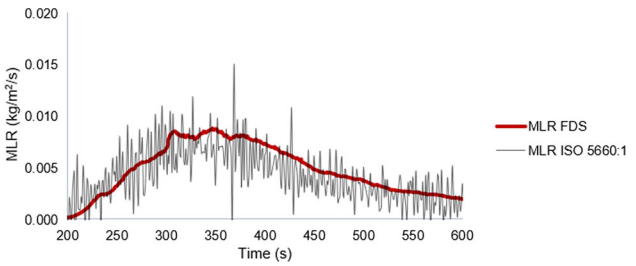

Fig. 6 FDS predicted MLR (red line) vs cone calorimeter MLR recordings (black lines) (Color figure online)

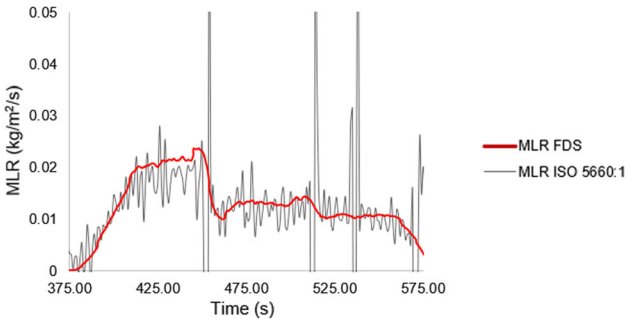

Fig. 7 Cone calorimeter experimental MLR recordings (black lines) vs FDS predicted MLR (red line) (Color figure online)

observed (Table 2), with visibly enhanced material degradation of the outer aluminium-alloy facing (Fig. 5).

Visibly enhanced material degradation of the outer aluminum-alloy facing for sample with water spray (Fig. 5).

The average heat of combustion value recorded increased from 43.1 to 60.3 MJ/kg (Table 2). However, it is suspected that the value was inflated by either oxidation of exposed aluminum, or the hydration of CaO, resulting in mass gain, causing an imbalance in the true mass loss/total heat release calculation used to determine heat of combustion.

Initial exothermic response (Fig. 4), up to a heat release rate of 7.2 kW/m^2, is observed for the sample sprayed with water. Relative to overall heat release curve, this is an insignificant value. However, resulting mechanical damage affected dynamic heat release rate.

Experimental heat release rate data for the sample exposed to water spray correlate closely with predicted values, based on ethylene-only fuel. Evidence of hydrogen causing an increase in pHRR is not supported.

In summary, the enhanced mechanical degradation observed on the aluminum facing indicates thermal shock mechanisms occurred. However, aluminum's contribution to overall combustion of the sample, through either H_2 liberation, or combustion of the metal, is found to be negligible.

Therefore, the current findings of this study are not in agreement with the hypothesis investigated. However, further investigation is required to identify the precise mechanisms involved. It is also of interest to determine the significance of enhanced degradation of aluminum facings brought upon by environmental conditions, as well as the behavior and effects of $CaCO_3$ used as a filler for PE blends. This will assist in developing the current understanding and dynamic time-dependent modeling of ACMs behavior during façade fires, highlighting the potential for unforeseen hazards.

Acknowledgments The authors would like to thank Kingspan Holdings (IRL) Ltd. for their support toward a Ph.D. project at the University of Portsmouth.

References

1. M. Bonner, G. Rein (2020) List of facade fires 1990–2020. https://doi.org/10.5281/ZENODO.3743863
2. A. Khan, S. Lin, X. Huang, A. Usmani, Facade fire hazards of bench-scale aluminum composite panel with flame-retardant core. Fire Technol. (2021). https://doi.org/10.1007/s10694-020-01089-4
3. E. Guillaume, V. Dréan, B. Girardin et al., Reconstruction of Grenfell Tower fire. Part 1: lessons from observations and determination of work hypotheses. Fire Mater. **44**, 3–14 (2020). https://doi.org/10.1002/fam.2766
4. E. Guillaume, V. Dréan, B. Girardin et al., Reconstruction of Grenfell Tower fire. Part 2: a numerical investigation of the fire propagation and behaviour from the initial apartment to the façade. Fire Mater. **44**, 15–34 (2020). https://doi.org/10.1002/fam.2765
5. E. Guillaume, V. Dréan, B. Girardin et al., Reconstruction of Grenfell Tower fire. Part 3—Numerical simulation of the grenfell tower disaster: contribution to the understanding of the fire propagation and behaviour during the vertical fire spread. Fire Mater. **44**, 35–57 (2020). https://doi.org/10.1002/fam.2763
6. V. Dréan, B. Girardin, E. Guillaume, T. Fateh, Numerical simulation of the fire behaviour of façade equipped with aluminium composite material-based claddings—model validation at intermediate scale. Fire Mater. **43**, 839–856 (2019). https://doi.org/10.1002/fam.2745
7. V. Dréan, B. Girardin, E. Guillaume, T. Fateh, Numerical simulation of the fire behaviour of facade equipped with aluminium composite material-based claddings-model validation at large

scale. Fire Mater. **43**, 981–1002 (2019). https://doi.org/10.1002/fam.2759
8. Silva JCG, Landesmann A, Ribeiro FLB (2014) Interface model to fire-thermomechanical performance-based analysis of structures under fire conditions. Fire Evacuation Model Tech Conf 2014
9. S.T. McKenna, N. Jones, G. Peck et al., Fire behaviour of modern façade materials—understanding the Grenfell Tower fire. J Hazard Mater. **368**, 115–123 (2019). https://doi.org/10.1016/j.jhazmat.2018.12.077
10. A.A. Stec, K. Dickens, J.L.J. Barnes, C. Bedford, Environmental contamination following the Grenfell Tower fire. Chemosphere. **226**, 576–586 (2019). https://doi.org/10.1016/j.chemosphere.2019.03.153
11. J. Schulz, D. Kent, T. Crimi et al., A critical appraisal of the UK's regulatory regime for combustible façades. Fire Technol. **57**, 261–290 (2021). https://doi.org/10.1007/s10694-020-00993-z
12. G. Srivastava, D. Nakrani, C. Ghoroi, Performance of combustible facade systems with glass, ACP and firestops in full-scale, real fire experiments. Fire Technol. **56**, 1575–1598 (2020). https://doi.org/10.1007/s10694-019-00943-4
13. Aluminium Association (2020) Annual Summary Report on molten metal incidents for 2019/20. https://www.aluminum.org/sites/default/files/2020 Molten Metal Incident Annual Summary Report 092120.pdf. Accessed 21 Jun 2021
14. British Standard Institution (2020) BS EN ISO 1182:2020 Reaction to fire tests for products. Non-combustibility test. https://shop.bsigroup.com/ProductDetail?pid=000000000030338547. Accessed 6 Jun 2021
15. ASTM International (2019) ASTM E136-19a, Standard Test Method for Assessing Combustibility of Materials Using a Vertical Tube Furnace at 750°C. https://www.astm.org/Standards/E136.htm. Accessed 17 Jul 2021
16. Harper C, Gomez C (2011) Fire performance evaluation tested in accordance with ASTM E136-11, standad test method for behavior of materials in a vertical tube furnace at 750C: Material ID and Trade Name: 5052
17. Aluminium Association (2020) Alloy combustibility test reports
18. Nadj D (2019) Deregulation, the absence of the law and the Grenfell tower fire. In: Queen Mary Hum. Rights Law Rev. https://www.qmul.ac.uk/law/humanrights/media/humanrights/docs/Nadj-final.pdf. Accessed 14 Aug 2021
19. Adams L (2017) Professor Laurence Harwood from the University of Reading tested materials to help the Grenfell Tower Inquiry. In: Read. Chron. https://www.readingchronicle.co.uk/news/15570964.professor-laurence-harwood-from-the-university-of-reading-tested-materials-to-help-the-grenfell-tower-inquiry/. Accessed 14 Jun 2021
20. Maguire J, Woodcock L (2018) Thermochemistry of Grenfell tower fire disaster: catastrophic effects of water as an "Extinguisher" in aluminium conflagrations
21. J.F. Maguire, L.V. Woodcock, Thermodynamics of tower-block infernos: effects of water on aluminum fires. Entropy. **22**, 14 (2020)
22. Maguire J, Woodcock L (2021) Grenfell fire scientific timeline. https://www.researchgate.net/publication/349692532_Grenfell_Fire_Scientific_Timeline. Accessed 14 Jul 2021
23. Taleyarkhan RP, Kim SH, Knaff C (2001) Fundamental studies on molten aluminum-water explosion prevention in direct-chill casting pits. Light Met Proc Sess TMS Annu Meet (Warrendale, Pennsylvania) 793–798
24. León DD, Richter RT, Levendusky TL (2016) Investigation of coatings which prevent molten aluminum/water explosions BT—essential readings in light metals: volume 3 cast shop for aluminum production. In: Grandfield JF, Eskin DG (eds). Springer, Cham, pp 1068–1073
25. G. Li, H.X. Yang, C.M. Yuan, R.K. Eckhoff, A catastrophic aluminium-alloy dust explosion in China. J Loss Prev Process Ind. **39**, 121–130 (2016). https://doi.org/10.1016/j.jlp.2015.11.013
26. A. Andreozzi, N. Bianco, M. Musto, G. Rotondo, Parametric analysis of input data on the CFD fire simulation. J. Phys. Conf. Ser. (2019). https://doi.org/10.1088/1742-6596/1224/1/012011
27. Hakkarainen T (2002) Studies on fire safety assessment of construction products. VTT Publ 3–109
28. The International Organization for Standardization (2015) Reaction-to-fire tests—Heat release, smoke production and mass loss rate—Part 1: Heat release rate (cone calorimeter method) and smoke production rate (dynamic measurement) ISO 5660-1:2015. https://www.iso.org/standard/57957.html. Accessed 4 Jun 2021
29. ASTM E1354-17, Standard Test Method for Heat and Visible Smoke Release Rates for Materials and Products Using an Oxygen Consumption Calorimeter, ASTM International, West Conshohocken, PA, 2017, www.astm.org
30. K. McGrattan, S. Hostikka, R. McDermott, et al., Sixth Edition Fire Dynamics Simulator User 's Guide (FDS). NIST Spec Publ 1019 Sixth Edit: (2020)
31. Thunderhead engineering (2015) PyroSim User Manual. In: Building. https://www.thunderheadeng.com/wp-content/uploads/dlm_uploads/2014/02/PyroSimManual.pdf. Accessed 20 Aug 2021
32. The International Organization for Standardization (2014) Plastics—Thermogravimetry (TG) of polymers—Part 1: General principles
33. The International Organization for Standardization (2014) ISO 11358-2:2014 Plastics—Thermogravimetry (TG) of polymers—Part 2: Determination of activation energy. https://www.iso.org/standard/65086.html. Accessed 18 Jul 2021
34. The International Organization for Standardization (2013) ISO 11358-3:2013 Plastics—Thermogravimetry (TG) of polymers—Part 3: determination of the activation energy using the Ozawa-Friedman plot and analysis of the reaction kinetics. https://www.iso.org/standard/54366.html. Accessed 18 Jul 2021
35. G.M. Scamans, P.R. Andrews, C. Butler et al., Surface treatment of aluminium automotive sheet: mythology and technology. Surf Interface Anal. **45**, 1430–1434 (2013). https://doi.org/10.1002/sia.5279
36. K. McGrattan, S. Hostikka, R. McDermott, et al., Sixth Edition Fire Dynamics Simulator User 's Guide (FDS). In: NIST Spec. Publ. 1019 (2020)
37. K. McGrattan, S. Hostikka, R. McDermott, et al., Sixth edition fire dynamics simulator technical reference guide Volume 1: Verification guide. 1:1–147 (2021)
38. C. Lautenberger, G. Rein, C. Fernandez-Pello, The application of a genetic algorithm to estimate material properties for fire modeling from bench-scale fire test data. Fire Saf J. **41**, 204–214 (2006). https://doi.org/10.1016/j.firesaf.2005.12.004